Research

Analysis of Polyubiquitin Conjugates Reveals That the Rpn10 Substrate Receptor Contributes to the Turnover of Multiple Proteasome Targets*⑤

Thibault Mayor, J. Russell Lipford, Johannes Graumann, Geoffrey T. Smith, and Raymond J. Deshaies‡

The polyubiquitin receptor Rpn10 targets ubiquitylated Sic1 to the 26S proteasome for degradation. In contrast, turnover of at least one ubiquitin-proteasome system (UPS) substrate, CPY*, is impervious to deletion of *RPN10*. To distinguish whether *RPN10* is involved in the turnover of only a small set of cell cycle regulators that includes Sic1 or plays a more general role in the UPS, we sought to develop a general method that would allow us to survey the spectrum of ubiquitylated proteins that selectively accumulate in *rpn10Δ* cells. Polyubiquitin conjugates from yeast cells that express hexahistidine-tagged ubiquitin (H$_6$-ubiquitin) were first enriched on a polyubiquitin binding protein affinity resin. This material was then denatured and subjected to IMAC to retrieve H$_6$-ubiquitin and proteins to which it may be covalently linked. Using this approach, we identified 127 proteins that are candidate substrates for the 26S proteasome. We then sequenced ubiquitin conjugates from cells lacking Rpn10 (*rpn10Δ*) and identified 54 proteins that were uniquely recovered from *rpn10Δ* cells. These include two known targets of the UPS, the cell cycle regulator Sic1 and the transcriptional activator Gcn4. Our approach of comparing the ubiquitin conjugate proteome in wild-type and mutant cells has the resolving power to identify even an extremely inabundant transcriptional regulatory protein and should be generally applicable to mapping enzyme substrate networks in the UPS. *Molecular & Cellular Proteomics 4:741–751, 2005.*

In eukaryotic cells, protein degradation plays a critical role in the regulation of a variety of cellular processes including the cell cycle, apoptosis, signal transduction, and gene expression. The ubiquitin-proteasome system (UPS)[1] is the principal pathway that targets proteins for degradation. In this pathway, proteins to be degraded are marked by covalent modification of a lysine residue with an ubiquitin chain. The enzymatic reaction (ubiquitylation) is driven by an ubiquitin-activating enzyme E1, ubiquitin-conjugating enzyme E2, and ubiquitin-ligase E3 (1). The substrate conjugated to the ubiquitin chain is then recognized by the 26S proteasome and degraded. The exquisite specificity of substrate recognition for ubiquitylation is thought to be determined primarily by E3, which binds specifically to substrate (2, 3). The budding yeast genome encodes about 50 putative ubiquitin-ligases,[2] whereas metazoans may have more than 400 (4). Because each ubiquitin-ligase presumably can target several substrates, ubiquitylation represents one of the main post-translational modifications in the cell. Therefore, deciphering the network of enzyme-target interactions in the UPS will be a major undertaking.

To be recognized by the proteasome, a substrate-linked ubiquitin chain must assemble through lysine 48 (Lys^{48}) of ubiquitin (5). By contrast, mono-ubiquitin linkages and multiubiquitin chains linked via the alternative lysine 63 (Lys^{63}) of ubiquitin regulate multiple pathways by nonproteolytic means, including DNA repair (6), chromatin topology, and vesicle trafficking (7). In the past few years, several proteins that recognize specifically Lys^{48}-linked chains have been identified. Rpn10, a stoichiometric component of the 26S proteasome, was the first protein shown to bind polyubiquitin chains (8). Rpn10 harbors two characterized domains: the amino-terminal von Willebrand A (VWA) domain that mediates proteasome association and the carboxyl-terminal ubiquitin-interacting motif (UIM) domain. The UIM is also present in other proteins involved in the ubiquitin pathway and endocytosis (9). Based on its ability to bind to the proteasome and to ubiquitylated proteins, Rpn10 was predicted to be the major proteasome receptor for ubiquitylated substrates. However, deletion of *RPN10* in budding yeast is not lethal, indicating that other proteins must act as proteasome receptors (10). Rad23 and Dsk2 belong to a second group of proteins that

[1] The abbreviations used are: UPS, ubiquitin-proteasome system; UIM, ubiquitin-interacting motif; UBA, ubiquitin-associated; UB, urea buffer; TAP, tandem affinity purification.

[2] T. Mayor and R. J. Deshaies, unpublished data.

interacts with the proteasome via an amino-terminal ubiquitin-like domain and contain a carboxyl-terminal polyubiquitin binding motif, the ubiquitin-associated (UBA) domain. There is evidence suggesting that both proteins can act as proteasome receptors (11, 12). There is also other evidence that suggests these two proteins may play an alternative role in protecting ubiquitylated substrates from de-ubiquitylation activity and in promoting or in inhibiting multiubiquitylation of substrates (13–16). Whereas the physiological functions of ubiquitin binding proteins remain to be fully elucidated, a recent study showed that mutations in *RPN10*, *RAD23*, or *UFD1* (Ufd1 is a member of a protein complex that may also act as a proteasome substrate receptor) selectively impair the turnover of distinct substrates of the UPS (17). This surprising finding implies that different targeting mechanisms are used by the proteasome to degrade specific subsets of substrates. Certain UPS substrates (Sic1, Clb2, and Gic2) but not others (CPY* and the Deg1 degron of Matα2) are strongly influenced by Rpn10 (17). This suggested that a restricted class of UPS substrates, possibly short lived regulators of the cell cycle and its efferent pathways, is targeted to the proteasome by Rpn10.

Here, we employ a new method for ubiquitin conjugate affinity purification to identify proteins that accumulate as ubiquitylated species in yeast cells that lack Rpn10. Our analysis greatly expands the role that Rpn10 plays in protein turnover *in vivo*. By applying the approach described here, it should be possible to systematically identify the constellation of substrates targeted to the proteasome by each individual receptor pathway in *Saccharomyces cerevisiae*.

EXPERIMENTAL PROCEDURES

Yeast Strains and Plasmids—All *S. cerevisiae* strains used in this study are listed in supplemental Table 1. RJD2997 was generated by integrating the plasmid RDB1848, which contains the coding sequences for H_6-ubiquitin flanked by the GPD constitutive promoter and PGK terminator sequences (18), into the *TRP1* locus. Control strain RJD2998 was obtained by integrating the empty vector into the *TRP1* locus. Mutant *rpn10Δ* was retrieved from the Yeast Deletion Library (Open Biosystem) and back-crossed into the W303 background. Gcn4-Myc9 was previously described (19). S288C strains with TAP-tagged genes were retrieved from the Yeast TAP-Fusion Library (Open Biosystem).

The H_8-ubiquitin coding sequence was placed between the GPD constitutive promoter and PGK terminator sequences in pRS316 (RDB1851). A pair of primers (5′-GCGGATCCATGAGAGGTAGTCAC-CACCATCATCACCATCATCACGGTGGTATGCAGATTTTCG-3′ and 5′-GAGCTCGAGACCACCTCTTAGCCTTAGCAC-3′) was used to amplify by PCR yeast ubiquitin (the first repeat of the *UBI4* locus). The PCR fragment was digested with BamHI and XhoI and ligated into the yeast expression vector pG-1 (20) (digested with BamHI and SalI). An EcoRI-NaeI fragment containing H_8-ubiquitin was then ligated into pRS316 (digested with EcoRI and SmaI).

Immobilization of Polyubiquitin Binding Proteins—GST-Rad23 and GST-Dsk2 were generous gifts from H. Kobayashi and H. Yokosawa, respectively. Fusion proteins were expressed in BL21(DE3)/pLysS and purified using glutathione-Sepharose resin. Ten mg of GST-Dsk2p and 20 mg of GST-Rad23 were separately coupled to 1.5 ml of resin volume of CNBr-activated Sepharose 4B (Amersham Biosciences) in 100 mM NaHCO₃, pH 8.3, 0.5 M NaCl. Coupled resin was stored at 4 °C in a 50% slurry with 100 mM Tris-HCl, pH 8.0, 0.5 M NaCl, 0.02% NaN₃.

Two-step Purification—Cells were grown in 6 liters of YPD medium (2% peptone, 1% yeast extract, 2% dextrose) at 25 °C to an A_{600} of 1.5. Cells were washed with 1/6 volume of ice-cold TBS followed by 1/30 volume of ice-cold TBS with 1 mM 1,10-phenanthroline, 10 mM iodoacetamide. Cells were lysed using a One Shot Cell Disrupter (Constant Systems) at 30,000 psi in 40 ml of lysis buffer (300 mM NaCl, 0.5% Triton X-100, 50 mM sodium phosphate, pH 8.0, 0.5 mM AEBSF, 5 μg/ml aprotinin, 5 μg/ml chymostatin, 5 μg/ml leupeptin, 1 μg/ml pepstatin A, 1 mM 1,10-phenanthroline, 10 mM iodoacetamide). Lysate (typically 1.5 g of protein) was cleared by centrifugation at 4 °C in a Sorvall SS34 for 20 min at 14,000 rpm. Two milligrams each of GST-Rad23 and GST-Dsk2 coupled to Sepharose (pre-equilibrated with lysis buffer) were added to the clarified lysate and mixed for 90 min at 4 °C. The resin was then washed with 40 ml of lysis buffer, further mixed for 15 min with 20 ml of 50 mM sodium phosphate, pH 8.0, 2 M NaCl, and washed once with 20 ml of 50 mM sodium phosphate, pH 8.0, 2 M NaCl and twice with 20 ml of 50 mM sodium phosphate, pH 8.0, 300 mM NaCl, 0.1% Triton X-100. Elution was performed at room temperature with two successive incubations with 1 ml of urea buffer (UB: 8 M urea, 100 mM NaH₂PO₄, 10 mM Tris-HCl, pH 8.0), and imidazole was added to a final concentration of 20 mM. Eluate was then mixed with 125 μl of nickel magnetic bead slurry (Promega V8565, prewashed in the UB) for 60 min on a rotating wheel. The beads were washed with 1 ml of UB and mixed for 15 min with UB supplemented with 0.5% SDS. The beads were then washed with 1 ml of UB with 0.5% Triton X-100 and mixed for 15 min with another 1 ml of UB with 0.5% Triton X-100. The last procedure was repeated using UB only.

To generate peptides for MS-based sequencing, we performed the tryptic digest directly on the beads. The beads were incubated with 500 μl of UB with 3 mM Tris-(2-carboxyethyl)phosphine (T-CEP) for 20 min and then for another 15 min following addition of iodoacetimide to 11 mM. The buffer volume was reduced to 75 μl by removing excess liquid, and 0.2 μg of endoproteinase Lys-C (Roche) was added. Beads were incubated at 37 °C with intermittent shaking for 5 h. Dilution buffer (225 μl of 100 mM Tris-HCl, pH 8.0, 1.33 mM CaCl₂) was then added followed by 1 μg of trypsin (Roche Applied Science), and the beads were further incubated with intermittent shaking for 16 h at 37 °C. The supernatant was carefully collected, and formic acid was added to a final concentration of 5%.

MS and Data Analysis—The proteolytically digested sample was further processed for multidimensional chromatography coupled in-line to ESI-MS as described previously (21). As a variation to the chromatography program, samples were stepped off the strong cation exchanger phase of the triphasic column using 12.5, 20, 30, 40, and 100% buffer C (500 mM ammonium acetate, 5% ACN, 0.1% formic acid). Centroided fragmentation spectra acquired by Xcalibur 1.3 (ThermoElectron) were evaluated for spectrum quality and charge state using 2to3 (22) and searched against the translated open reading frames of the *Saccharomyces* Genome Database (SGD (23); release time stamp: 07/26/2004; 6,860 entries) with Sequest (version 27, revision 9; Ref. 24) utilizing unified input and output files (25). Relevant Sequest parameters used were: (i) peptide mass tolerance of 3.0 amu, (ii) parent ion masses were treated as monoisotopic, (iii) fragmentation ion masses were treated as averaged, and (iv) a 57.0-amu static modification on cysteines accounted for alkylation. Sequest results were filtered using DTASelect 1.9 and Contrast (26) with the following requirements for peptide and locus identifications considered valid: minimum Xcorrs of 1.8, 2.5, and 3.5 for singly, doubly, and triply charged ions, respectively; a minimum ΔCn of 0.08; and a

minimum of two valid peptides per locus.

Small Scale Cell Extraction, IMAC, and Western Blotting—For direct comparison of protein level in wild-type and *rpn10Δ* strains, S288C cells were grown in YPD at 25 °C until an A_{600} of 0.5–1 was reached. An amount of yeast cells corresponding to 4–5 A_{600} was collected, briefly washed with 1 ml of 1× TBS, and frozen in liquid nitrogen. Cells were directly resuspended in prewarmed sample buffer, incubated for 2 min at 96 °C, lysed with glass beads in a FastPrep 120 (Thermo Savant) for 45 s with a speed setting of 5.5, and incubated for another 4 min at 96 °C. For IMAC purification of H_8-ubiquitin, cells transformed with a *URA3*-based plasmid coding for H_8-ubiquitin were grown in 100 ml of SD-URA medium (0.67% yeast nitrogen base, 5% dextrose) at 30 °C to an A_{600} of 1. TCA (20% final) was added directly to the cell culture, and cells were incubated for 10 min on ice and washed with ice-cold 100 mM Tris-HCl (once with pH 8.5, twice with pH 8.0). Cells were resuspended in 0.6 ml of 0.2% SDS, 8 M urea, 100 mM Hepes, pH 8.0, 1 mM 1,10-phenanthroline, 5 mM *N*-ethylmaleimide (NEM), 0.5 mM AEBSF, 5 μg/ml aprotinin, 5 μg/ml chymostatin, 5 μg/ml leupeptin, 1 μg/ml pepstatin A, and lysed by agitation with glass beads in a FastPrep 120. Glass beads were further washed with 0.6 ml of lysis buffer without SDS, and lysate (containing 0.1% SDS) was cleared 10 min at 14,000 rpm in a microcentrifuge. Imidazole (20 mM final) and nickel magnetic beads (70 μl) were added to 8.5 mg of lysate protein and mixed for 1 h at room temperature. Beads were then washed three times in 0.1% SDS, 8 M urea, 100 mM Hepes, pH 8.0, and proteins were eluted in SDS-PAGE sample buffer supplemented with 1 M imidazole, 4 M urea, 50 mM Hepes, pH 8.0. TAP-tagged proteins were detected using the anti-calmodulin binding peptide antibody (Upstate Biotechnology), ubiquitin with MAB1510 (Chemicon International), Cdc28 with PSTAIR antibody (Santa Cruz Biotechnology), and Gcn4-Myc9 with 9E10 monoclonal antibody.

RESULTS

Two-step Purification of Ubiquitin Conjugates—We performed two-step purification of ubiquitin conjugates (Fig. 1) from cells that express ubiquitin fused to an amino-terminal hexahistidine tag (H_6-ubiquitin), and as control we repeated the procedure with cells that do not express H_6-ubiquitin. In both experiments, the first purification step yielded a similar amount of proteins, whereas the IMAC only recovered appreciable material from the H_6-ubiquitin strain (Fig. 2*A*). The signal revealed by silver staining of material fractionated by SDS-PAGE ranged from 50 to 250 kDa and produced a spread rather than discrete bands, as expected for a large collection of different proteins conjugated to ubiquitin chains of various lengths. We calculated that the first step in purification recovered about 15% of the polyubiquitin conjugates in the cell (Fig. 2*B*). Notably, mono-, di-, and triubiquitin species were not recovered. This implies that the UBA domains of Rad23 and Dsk2 were only enriching for proteins conjugated to ubiquitin chains that contained more than three ubiquitins. Because a tetraubiquitin chain is thought to comprise the minimal signal for targeting substrates to the proteasome for degradation (27, 28), the UBA affinity step appears to enrich specifically for those ubiquitin conjugates that are proteasome substrates. In the second step, the majority of the ubiquitin conjugates (>80%) eluted from the first resin were recovered (Fig. 2*C*). In this experiment, only 25–30% of the
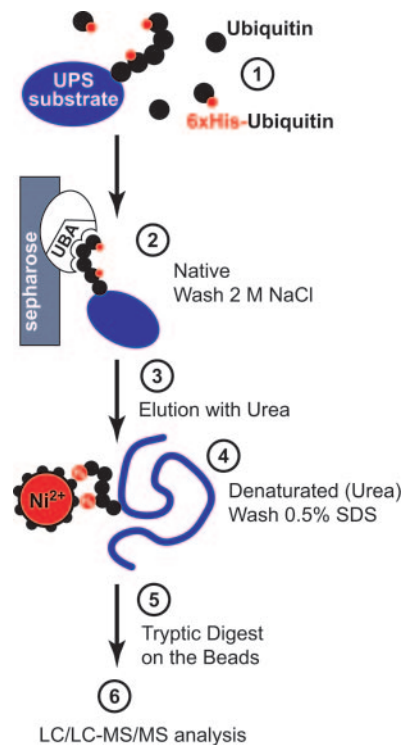
FIG. 1. **Flow diagram for the two-step purification of polyubiquitin conjugates.** Yeast cells that constitutively express ubiquitin modified with an amino-terminal hexahistidine tag are lysed in nondenaturing buffer (*1*). Polyubiquitin chains are purified using matrices derivatized with the recombinant UBA domain-containing proteins Rad23 and Dsk2. UBA domains bind tightly to multiubiquitin chains, with a preference for chains linked via lysine 48 of ubiquitin (11, 49). Contaminant proteins are removed by washes with 2 M NaCl (*2*), and specifically bound proteins are then eluted in 8 M urea (*3*) and mixed with nickel magnetic beads (*4*). In this second purification step, stringent washing conditions (0.5% SDS) are used to remove contaminants. Trypsin is then applied directly to the beads (*5*), and peptides released from the beads are analyzed by LC/LC-MS/MS (*6*).

bound material was eluted with sample buffer from the nickel beads (data not shown). Overall, our procedure resulted in a 3,000- to 5,000-fold enrichment of polyubiquitin conjugates (1,500 mg of protein extract resulted in 30–50 μg of protein, representing 10% of the polyubiquitin in the cell).

MS Analysis—Purified proteins were directly digested on the nickel beads, and the peptide mixture was analyzed by multidimensional LC-MS/MS or MudPIT. Sequest and DTASelect algorithms were used to analyze the spectra generated by the complex mixture of affinity-purified proteins, and 180 nonredundant proteins were identified (supplemental Table 2). The most abundant protein in our analysis was ubiquitin. Of a total of 5,347 sequencing events, 457 peptides derived from ubiquitin. This was expected because ubiquitin should be the most prominent protein after the purification. For clarity, we further filtered our data by removing transposon-related genes, duplicated genes, ubiquitin fusion genes, and Rad23 and Dsk2 that leached from the resin used in the first purification step (data not shown). The 127 remaining proteins are
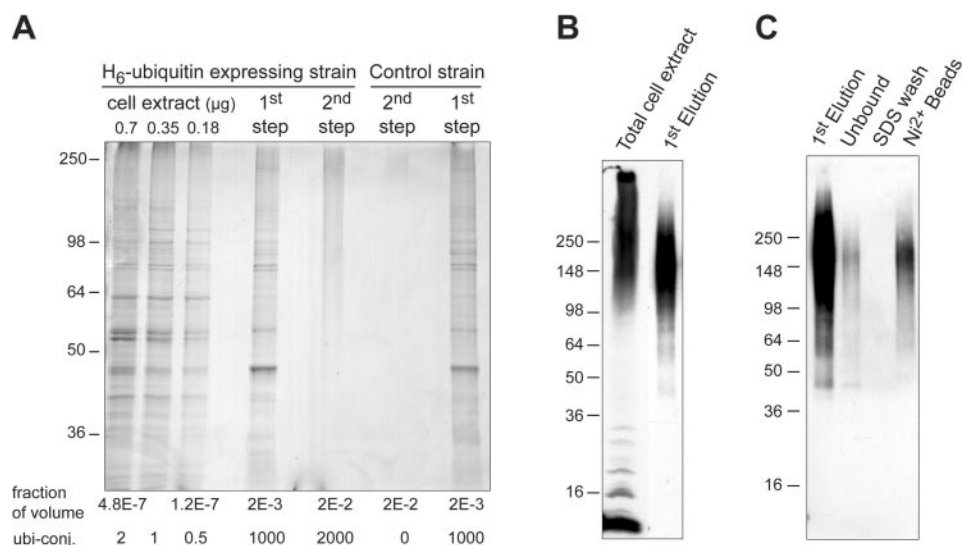
Fig. 2. **Two-step affinity purification specifically enriches for polyubiquitylated proteins.** *A*, SDS-PAGE analysis of the two-step purification. Purifications were performed using the H_6-ubiquitin-expressing strain or the wild-type control strain that lacks tagged ubiquitin. Aliquots of total cell extract, proteins eluted after the first step (UBA affinity) of the purification, and proteins from the second step (those bound to the nickel magnetic beads) were separated by SDS-PAGE on a 10% polyacrylamide gel and stained with silver. Amounts loaded in comparison to initial volumes are indicated immediately below each lane. Below that, the amount of ubiquitin conjugates for each lane (as estimated by Western blotting, data not shown) is indicated in arbitrary units. *B*, immunoblotting of the first purification step. Aliquots of total cell extract and the eluate from the UBA domain affinity step (first elution) were separated by SDS-PAGE on a 4–20% polyacrylamide gradient gel and immunoblotted with an anti-ubiquitin antibody. The sample from the first elution is overloaded 10-fold relative to the total cell extract. *C*, immunoblotting of the IMAC purification step. Equal portions of initial volumes corresponding to proteins that were eluted from the UBA domain matrix, failed to bind the nickel-based matrix (unbound), were washed away with 0.5% SDS (SDS wash), or bound to the nickel beads (Ni^{2+} beads) were processed as in *B*.

listed in Table I. We classified these proteins in different categories according to their function (Fig. 3*A*). The majority of identified proteins is involved in metabolism and translation. Several proteins are components of regulated pathways, and several were previously shown to be targets for degradation. These include Ole1, a short lived protein (29), Rpo21, which is ubiquitylated by Rsp5 (30), and Gdh1 and Mdh2, which were shown previously to be targeted for proteolysis (31, 32). Moreover, the list includes proteins for which ubiquitylation sites were previously identified; 14 of our 127 proteins were among the 71 identified in the initial global study of ubiquitylated proteins (33), and 8 of our 127 proteins were among the 33 found in a screen for membrane-associated ubiquitylated proteins (34). Thus, although we identified only ~2% of the yeast proteome (127/~6,000), these proteins accounted for 21% of the ubiquitylated proteins identified by Gygi and co-workers (33, 34), a 10-fold enrichment.

Because our ultimate goal was to compare the pool of ubiquitylated proteins in wild-type and *rpn10Δ* cells, it was important to assess the variability of the MS analysis. The sample from the two-step purification described above had been split in half after the trypsin digest but prior to the MS analysis. When the second half of the sample was analyzed, we identified 176 proteins (supplemental Table 3). The two LC/LC-MS/MS analyses of the same sample were then compared using the Contrast algorithm (Fig. 3*B*). More than 80%

of the proteins identified in one analysis were found in the other analysis. We noticed that the variability was accounted for mainly by proteins identified by two peptides (as the loss of one peptide identification for a particular protein led to its exclusion from the analysis). When we also took into account proteins identified by only one peptide, ~95% of proteins identified by two peptides in either dataset were also identified by at least one peptide in the duplicate analysis (Fig. 3*B*). This indicated that there was some variation in the data analysis, albeit tolerable, arising from either the HPLC or mass spectrometer. Moreover, proteins defined by our minimum cutoff of two peptides (and thus possibly of low abundance in the purified sample) were disproportionately susceptible to being overlooked. Because many potential targets of interest might be in the inabundant category, we decided to perform our subsequent analyses in triplicate to ensure the identification of a maximum number of ubiquitin conjugates.

Impact of the Proteasome Substrate Receptor Rpn10 on the Pool of Ubiquitin Conjugates—Our key motivation for developing proteomic methods to identify ubiquitin conjugates on a global scale was to use the method to identify substrates/targets for ubiquitin ligase and isopeptidase enzymes and other specificity determining factors in the UPS. In particular, we sought to determine the breadth of the impact of Rpn10 on ubiquitin-dependent proteolysis. We reasoned that deletion of *RPN10* would prevent the degradation of

TABLE I

Proteins identified by LC/LC-MS/MS after two-step purification of ubiquitin conjugates

Name	Sequence coverage (%)	Peptide	Name	Sequence coverage (%)	Peptide	Name	Sequence coverage (%)	Peptide
SSA2[a]	61.5	43	RPS13	19.9	3	TDH1	9.6	3
RPL2A, B	57.1	17	RPS17A, B	19.9	2	ACT1	9.1	2
RPL21A, B	55.0	12	IML2	19.7	10	RPL34A, B	9.1	2
RPS7B	54.2	6	SRO9	19.6	4	SAN1	9.0	2
SSA1[a]	47.4	32	PMA1[b]	19.2	14	GPM1	8.9	2
RPL10	43.0	9	CIT2[a]	17.8	6	STI1	8.8	4
RPL3	42.9	20	GLN1[a,b]	17.8	6	RPT1	8.8	3
RPL15A	42.2	10	RPL4A, B	17.7	4	UBP6	8.6	5
RPS20[a,b]	42.1	8	ENO1	17.4	6	NOP4	8.3	4
ERG1[a,b]	41.7	19	PMA2	16.1	13	HSP82	7.9	7
NCE103	40.7	6	PGK1	16.1	8	UFD2	7.8	6
RPS4A, B[a]	40.6	11	DRE2	16.1	5	GPD2	7.7	2
RPS7A	40.0	5	RPS8A, B	15.5	2	ACS2[a]	7.6	2
RPL27A, B	37.5	6	BGL2	15.3	4	OLE1	7.6	3
RPS11A, B	37.2	10	SSA4	15.1	12	FAS1	7.5	13
RPL28	36.2	10	RPS6A, B	14.8	4	HSP42	7.5	2
AAH1	36.0	10	HSP150	14.7	3	HSP104[b]	7.4	5
RPL19A	34.9	11	ENO2	14.6	4	RPB2	7.1	6
VMA7	34.7	2	PNG1	14.6	5	FAA4	7.1	3
RPL8A	34.4	7	RPL11B	14.4	2	YMR210W	6.7	2
TEF1, 2	34.3	9	CBR1	14.0	4	HEF3	6.6	6
RPL15B	33.8	7	TDH2	13.9	4	YOR091W	6.2	2
GDH1[a]	33.5	15	ADH1	13.2	4	LYS1	6.2	2
RPA190	32.5	49	YLR407W	13.1	2	PHO84[a]	6.1	3
RPL1A, B	31.3	5	UBC6	12.8	2	RPF2	6.1	2
RPS26A	30.3	3	URA2	12.2	20	CDC48[a]	5.1	3
ERG11	29.8	17	UBP3	12.1	9	FKS1[b]	5.0	5
RPS1A, B	29.8	7	RPT2	12.1	4	KCC4	4.9	2
RPL24A, B	29.7	7	SSA3	12.0	9	TKL1	4.9	3
TDH3	29.5	6	MLF3	11.9	3	GAS1	4.5	2
RPS18A, B	28.8	5	ERG5[a]	11.7	4	SNF1	4.3	2
YEF3	28.7	24	YDJ1	11.7	3	RFC1	3.5	2
RPS27A, B	28.0	2	RPS3[a]	11.7	2	STP2	3.3	2
SIK1	27.8	9	SAM1	11.5	2	KAR2	3.1	3
SSB1, 2	27.7	12	RPA135	11.2	7	RPO21[b]	2.8	4
RPL6B	26.7	6	CBF5	10.6	3	KAP123	2.7	2
RPS12	26.6	3	GDH3	10.5	7	GSC2[a]	2.2	2
YBR071W	25.6	4	RPN1	10.3	10	CRM1	2.2	2
RPS5	25.3	3	RPL6A	10.2	2	RET1	1.6	2
EFT2, 1	25.2	15	HSC82	10.1	8	NUM1	1.2	2
HYP2	24.8	2	RPL32	10.0	2	TIP20	1.0	2
MDH2	21.7	7	VTC4	9.8	8			
RPL18A, B	21.5	5	PRE9[b]	9.7	2			

[a] Ubiquitylated proteins identified by Peng *et al.* (33).
[b] Ubiquitylated proteins identified by Hitchcock et al. (34).

substrates dependent on Rpn10 for turnover. These substrates would then accumulate as polyubiquitylated conjugates. To proceed, we collected and analyzed six independent samples; three were obtained from wild-type cells (supplemental Tables 2 and 4) and three others from *rpn10Δ* cells (supplemental Table 5). We compared the six datasets using the Contrast algorithm (Fig. 3*C*). The variability between the different datasets (~30%) was in general higher than previously observed between two identical samples (Fig. 3*B*). This was expected because it is essentially impossible to

grow cells, lyse cells, and carry out consecutive affinity purification steps in a manner that is perfectly precise. Nevertheless, to identify the candidate targets of Rpn10, proteins represented in any of three *rpn10Δ* samples but not in any *RPN10* sample were extracted and rank-ordered according to sequence coverage of the identified protein (Table II). What is particularly noteworthy is that the second highest ranked candidate in this subtractive screen of the entire *S. cerevisiae* proteome was the cell cycle regulator Sic1, which is ubiquitylated by the SCF[Cdc4] complex at the G1/S transition (35).
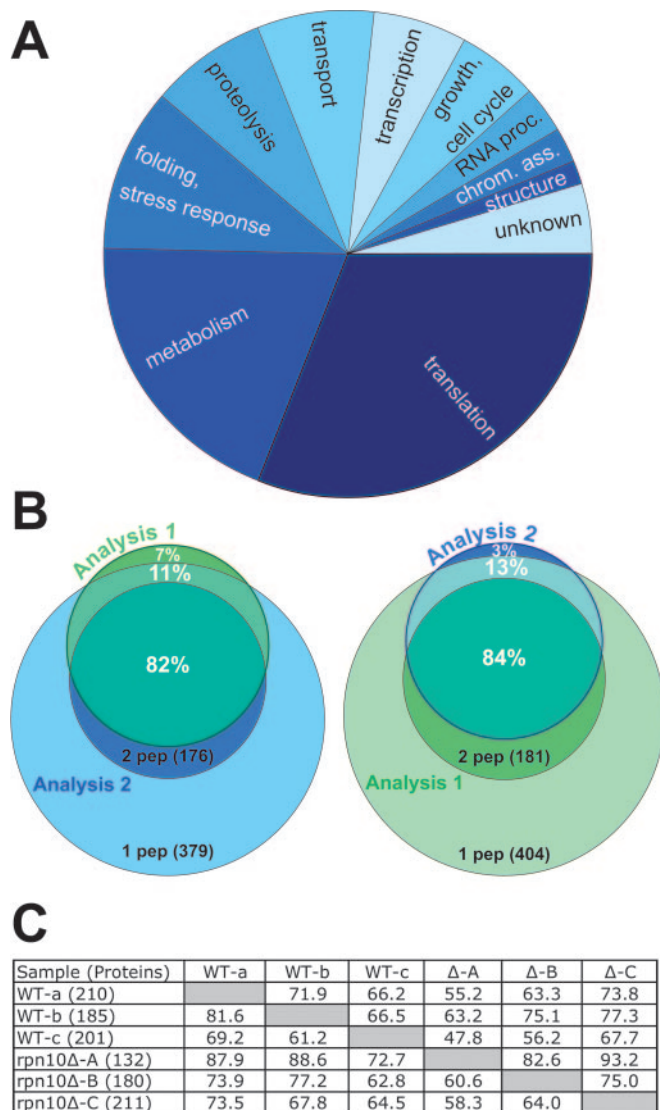
A

B

C

Sample (Proteins)	WT-a	WT-b	WT-c	Δ-A	Δ-B	Δ-C
WT-a (210)		71.9	66.2	55.2	63.3	73.8
WT-b (185)	81.6		66.5	63.2	75.1	77.3
WT-c (201)	69.2	61.2		47.8	56.2	67.7
rpn10Δ-A (132)	87.9	88.6	72.7		82.6	93.2
rpn10Δ-B (180)	73.9	77.2	62.8	60.6		75.0
rpn10Δ-C (211)	73.5	67.8	64.5	58.3	64.0	

FIG. 3. *A*, pie diagram of the identified proteins. Protein functions retrieved from the YPD database (Incyte) were plotted according to their representation in Table I. *B*, reproducibility of LC/LC-MS/MS analysis. *Left*, of 181 proteins identified by at least two peptides in *Analysis 1* (*green circle*), 82% were also identified by at least two peptides in *Analysis 2* (*dark blue circle*), 11% were identified by only one peptide in *Analysis 2* (*light blue circle*), and 7% were not recovered in *Analysis 2*. *Right*, same as *left*, except that the diagram indicates the percentage of the 176 proteins from *Analysis 2* (two peptide hits) that were identified at various levels of stringency in *Analysis 1*. *C*, pairwise analysis of the different samples (wild type and *rpn10Δ*). The percentage of proteins from one analysis (*row*) present in another analysis (*column*) is indicated. For each analysis, the number of identified proteins is shown in *parentheses*.

We had previously shown that Sic1 degradation is substantially dependent upon Rpn10 (17), suggesting that it is likely to accumulate as a ubiquitylated species in *rpn10Δ* cells (an assumption that was not addressed previously but has been validated as described below). Other candidates revealed by this substractive approach are also known to be targets for

ubiquitylation. The transcription factor Gcn4 is targeted for proteolysis after ubiquitylation by SCF[Cdc4] complex (19, 36, 37), and Aro10, Ald6, Erg3, and Ecm21 were identified as ubiquitylated proteins in a global analysis (33). Taken together, these findings suggest that our subtractive approach was sufficiently sensitive to identify critical regulatory targets of the UPS, even those of exceptionally low abundance such as Gcn4, which is estimated to be present at less than 50 molecules per cell (38).

Validation of Rpn10 Targets—To evaluate the role of Rpn10 in turnover of candidate substrates identified by our MudPIT approach, we assayed several of the proteins from Table II for abundance and ubiquitylation. First, we compared protein levels in *RPN10* and *rpn10Δ* strains in which the endogenous loci were modified to encode the candidate proteins with TAP tags fused to their C termini (Fig. 4*A* and Table II). For several candidates, protein levels were elevated in the *rpn10Δ* strain, suggesting that normal turnover of these proteins was Rpn10 dependent. For Gcn4, we employed a well characterized allele that encodes a carboxyl-terminal Myc9 tag integrated into the *GCN4* locus (19). We found that Gcn4 accumulated in *rpn10Δ* extracts, and we could also detect species migrating with a lower mobility that correspond to polyubiquitylated Gcn4 (Fig. 4*B*).

In addition to inabundant proteins like Gcn4, our analysis also identified highly abundant proteins as such the ribosomal subunit Rpl13B. However, by Western blotting we could not see any increase in the level of Rpl13B in *rpn10Δ* (data not shown). We reasoned that in this case perhaps only a small fraction of the protein pool was targeted for degradation, and thus the overall protein abundance was not altered in *rpn10Δ*. To test this, we devised a single-step purification with nickel beads using cells transformed with a plasmid that expressed ubiquitin with an octahistidine tag fused to the amino terminus (H_8-ubiquitin). Purified proteins were detected with the TAP tag antibody. An untagged *rpn10Δ* strain that expressed H_8-ubiquitin was used as a negative control and gave no signal in the Western blot (Fig. 4*C*). After performing the same procedure with a Sic1-TAP strain, we noticed the distinctive accumulation of high molecular mass Sic1 conjugates in *rpn10Δ* but not in *RPN10* cells that expressed H_8-ubiquitin (Fig. 4*C*). No signal was readily detected *rpn10Δ* cells not expressing the H_8-ubiquitin. Therefore, ubiquitylated Sic1 specifically accumulated in cells lacking Rpn10. Rpl13B showed similar behavior. Although there was some nonspecific binding of unmodified Rpl13B to the nickel beads (lower band present in all three lanes), Rpl13B species that migrated at high molecular masses (>250 kDa) were exclusively detected in *rpn10Δ* cells that expressed H_8-ubiquitin. Notably, species modified with one, two, and three ubiquitins were also detected in wild-type cells whenever H_8-ubiquitin was expressed. However Rpl13B was only detected by MS in samples from *rpn10Δ* cells. Therefore the species modified with one, two, and three ubiquitins that were also present in *RPN10* cells

TABLE II
Putative ubiquitylated proteins identified in rpn10Δ but not wild-type cells (54)

Proteins listed were identified (by a minimum of two valid peptides) in any of three independent analyses of rpn10Δ cells (A, B, and C) but not in any of the three independent analyses of control cells (RPN10). Sequence coverage is indicated in percentages for A, B, and C analyses and in the total column (corresponding to the sum of sequence coverage in the three experiments). The final validation status (+ or –) for Rpn10 targets is indicated in the first column. The score for the increase of protein level in *rpn10Δ and the presence of ubiquitylated species detected after IMAC in rpn10Δ* are indicated in the middle and last column, respectively. NT, not tested; 0, not validated; 1, validated; 2, ubiquitylated species were detected in both rpn10Δ and *RPN10* cells.

| Name	A	B	C	Total	Validation			Name	A	B	C	Total	Validation		
GCN4	22.4	22.4	32.4	35.9	+	1	1	RPL16B		8.1		8.1			
SIC1		32		32	+	1	1	VTS1			7.5	7.5			
VMA2			24.2	24.2				CPA1		7.5		7.5	–	0	2
PUP3	23.9			23.9				YLL012W			7.2	7.2			
YJR014W		23.2		23.2	–	0	0	FET3		6.8		6.8	–	0	NT
VHS2		17.2	9.6	22.9	+	0	1	LEU1			6.7	6.7			
RPL13A, B		22.6		22.6	+	0	1	MCH4			6.4	6.4			
LYS20			22.4	22.4				PPQ1			5.6	5.6			
RPS29A, B	19.6			19.6				VPS72		4.9		4.9	–	0	2
LYS21			19.5	19.5				LYS2	3.6		3.2	4.8			
PCL1	12.2	12.2	12.5	18.6				SGV1			4.7	4.7			
SEL1			17.6	17.6				ERG3			4.4	4.4			
RPL20A, B		16.3		16.3				MBP1		4.2		4.2	–	0	NT
RPL17A, B		15.8		15.8				REB1		4.1		4.1	+	1	NT
ARO10	7.7	3.3	6	15.3	+	1	2	ILV2			3.9	3.9			
NOG2			14.8	14.8				NSP1		3.9		3.9	–	0	0
TUB1			13.4	13.4				TUB2			3.3	3.3			
TOM22	13.2		13.2	13.2				YOR112W		3		3			
GAT2		10.5	3.8	12.3				SHQ1			2.8	2.8			
RTS3			11.4	11.4				ECM21		2.7		2.7	+	1	NT
DDR48		11.2		11.2				SIR4		2.7		2.7			
TSR1		5.7	4.6	10.3	–	0	0	CHS7		2.5		2.5			
ALK1			10	10				STP1	1.9		1.9	1.9			
UBX7			9.6	9.6				CDC39			1.9	1.9			
SSF2			9.5	9.5				MLP1		1.7		1.7	+	1	NT
NIP1			9.2	9.2				PSK2		1.1		1.1	+	1	NT
ALD6	2.4	8.6		8.6				MDN1		0.3		0.3	+	1	NT

most likely were not enriched in the two-step purification, as is the case for free (*i.e.* not substrate-linked) mono-, di-, and triubiquitin (Fig. 2*B*). Vhs2 protein level was also found unaltered in *rpn10Δ* cells (despite its relative low abundance), but ubiquitylated Vhs2 was detected after IMAC of extracts from *rpn10Δ* cells that expressed H_8-ubiquitin (Fig. 4*C*).

DISCUSSION

In this article, we describe a new approach to the purification and analysis of ubiquitin conjugates in the budding yeast *S. cerevisiae*. Our approach involves two affinity purification steps. The first step selects for ubiquitin chains that were able to bind recombinant UBA domain-containing proteins and thus were most likely competent to support degradation of attached proteins. In the second step, ubiquitin conjugates that contain H_6-ubiquitin were enriched by IMAC. Conjugates that survived the two enrichment steps were digested to yield peptides, which were separated by multidimensional chromatography and sequenced by MS/MS. This protocol enabled us to identify a collection of candidate ubiquitin-conjugated proteasome substrates. By performing a "subtractive" compari-

son of conjugates recovered from wild-type cells *versus rpn10Δ* cells that lack the proteasome substrate receptor Rpn10, we were able to identify a collection of proteins that accumulate selectively in *rpn10Δ* and thus are candidate ligands for Rpn10. This effort revealed that the pool of candidate Rpn10 ligands is much larger than appreciated previously from one-off analyses.

The approach described here differs from prior "proteome-wide" analyses of ubiquitin- (33, 34) and SUMO-conjugated proteins (39–44) in several important respects. First, we present data on replicate analyses. We found modest variation (~17%) in duplicate MS analyses of a single sample, but significant variations (~30%) when the entire affinity purification and LC/LC-MS/MS analysis were repeated. Performing replicate analyses is thus of considerable importance when comparing the ubiquitin conjugate proteome in different strains (*e.g.* wild type and *rpn10Δ*) to ensure that any differences seen are due to the mutation under study and are not simply a product of experimental variability. Performing replicate experiments also helps to ensure that an analysis is as thorough as possible. For example, some candidates that
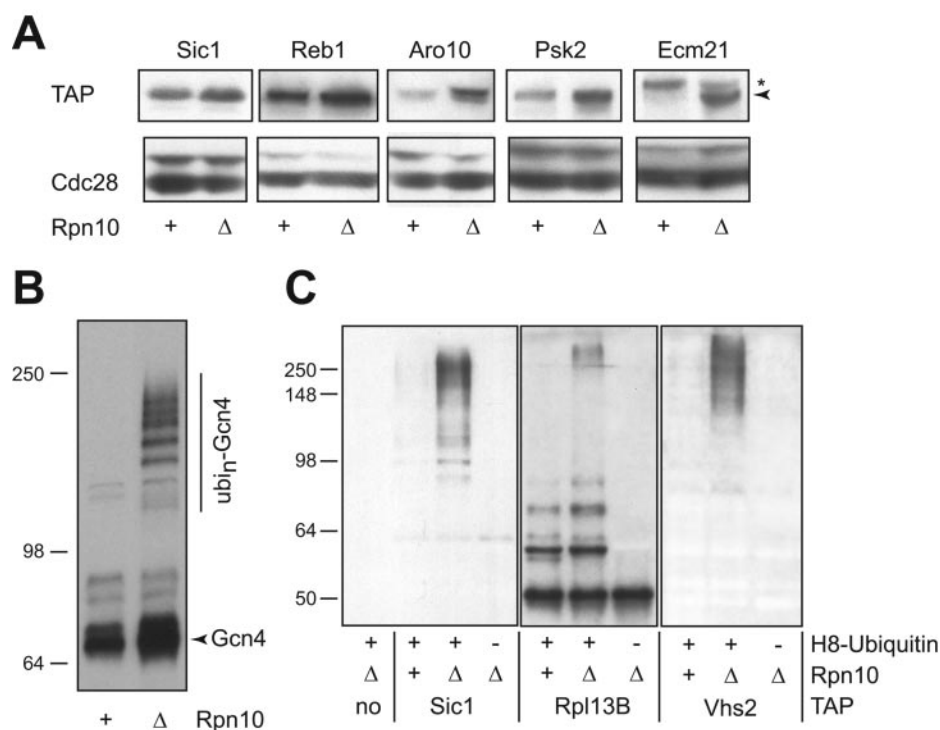
FIG. 4. **Analysis of candidate substrates of the Rpn10-dependent targeting pathway.** *A*, proteins whose level was increased in *rpn10Δ*. The chromosomal locus for each candidate investigated was modified to introduce a TAP epitope tag fused to the carboxyl terminus of the encoded protein. For each TAP-tagged candidate shown, equal amounts of proteins from *RPN10* (wild type) and *rpn10Δ* (Δ) cells were fractionated by SDS-PAGE on a 10% polyacrylamide gel and transferred to nitrocellulose. Immunoblotting was performed with anti-calmodulin binding peptide antibody that recognizes the TAP tag and anti-Cdc28 (which served as a loading control). The *caret* highlights a novel species of Ecm29 that was detected only in *rpn10Δ*. *B*, ubiquitylated Gcn4 accumulates in *rpn10Δ*. Equal amounts of proteins from *RPN10 GCN4[myc9]* and *rpn10Δ GCN4[myc9]* cells were separated by SDS-PAGE on a 10% polyacrylamide gel and transferred to nitrocellulose. Gcn4-Myc9 was detected using the 9E10 antibody. *C*, purification of proteins conjugated to H_8-ubiquitin. Proteins from strains with the indicated genotypes that bound nickel beads in buffer containing 8 M urea plus 0.1% SDS were loaded onto a 10% polyacrylamide gel and subjected to SDS-PAGE followed by immunoblotting with anti-calmodulin binding peptide antibody.

were validated (*e.g.* Sic1) were only identified in one of three analyses. Indeed, of the candidates for which identification was least robust (Mlp1, Psk2, and Mdn1, each of which was found in only one analysis at <2% sequence coverage), all three were validated as being responsive to Rpn10 function. Thus, we strongly recommend that multidimensional analyses be performed with replicate samples both to minimize false positives and to enhance identification of target proteins.

A second key difference is that we employed a "functional" affinity purification step in tandem with a tag-dependent affinity purification step. By comparison, Gygi and co-workers (33, 34) employed a single nickel-nitrilotriacetic acid affinity purification step in their analyses of the ubiquitin proteome. The inclusion of a second, function-based affinity step had two important consequences; first, it enabled superior enrichment for ubiquitin-conjugated proteins, and second, it focused our analysis on a particular subset of ubiquitin-conjugated proteins (*i.e.* those that are candidate substrates for the proteasome). In our hands, single-step purification with H_6-ubiquitin led to a relatively modest enrichment of ubiquitin conjugates (100- to 200-fold)[2] as compared with the two-step

purification (3,000- to 5,000-fold). This is in keeping with our experience that ~0.5% of total yeast extract proteins bind specifically to IMAC resins. Thus, it is possible that a fair fraction of the proteins identified previously are not *bona fide* UPS substrates. Importantly, our approach has permitted the identification of even the extremely inabundant UPS substrate Gcn4, which is present at less than 50 molecules per cell (38). Consistent with the greater degree of target focus intrinsic to our analysis, we did not identify proteins that are known to be conjugated with a single ubiquitin (*e.g.* histone H2A, B), nor did we enrich for mono-, di-, or triubiquitin chains (Fig. 2*B*). Finally, when we searched for peptides of ubiquitin itself that carried the Gly-Gly signature, Lys^{48} was found to be the most prominent conjugation site that was recovered (data not shown). Lys^{29}, Lys^{33}, and Lys^6 were more rarely identified, and modified Lys^{63} was not found. These findings suggest that we have established a new approach to identify specifically those proteins that are polyubiquitylated substrates of the proteasome. In the future, other ubiquitin receptors, like proteins containing UIM domains that bind mono-ubiquitylated targets in the endocytic pathway (*e.g.* Vps27 and Ent1)

or ZnF domains that bind selectively to Lys[63]-linked ubiquitin chains (45), may be used to identify factors in nonproteasomal pathways that are regulated allosterically by ubiquitylation.

Of the more than 120 proteins that we implicated as substrates of the UPS, most function in translational and metabolic pathways, and half of the candidates have high codon adaptation index values (>0.4).[3] Many ribosomal proteins were identified including some that were shown previously to be ubiquitylated, like Rpl28, Rps3, and Rps20 (33, 46). Because ribosomes are highly abundant and formed by tight macromolecular interactions, we cannot exclude that some of the identified proteins were contaminants. However, it is also possible that some of these candidate substrates might represent biosynthetic intermediates that fail to fold or assemble properly, resulting in their rapid degradation either during or shortly following the completion of translation (47, 48). In the latter case, one would predict that the UPS might have little impact on the total level of the candidate protein and that only a very small fraction of the total protein pool in the cell is ubiquitylated (depending on the fraction of the protein that misfolds or misassembles). This is exactly what we observed for Rpl13B. If a small fraction of Rpl13B fails to assemble properly and is degraded rapidly by the UPS, it could help to explain the presence of many proteins with high codon adaptation index values in our analysis. Thus, the bulk of proteins degraded by the proteasome in yeast cells might correspond to misfolded, damaged, or improperly translated proteins rather than proteins such as cyclins, CDK inhibitors, and transcription factors whose functions are regulated by proteolysis. Further studies will be required to address the important issue of substrate flux through the UPS in yeast. Notably, our method provides a means to identify substrates of the chaperone pathways that enable efficient protein folding and assembly as well as the ubiquitin ligases that target misfolded proteins for degradation by the UPS.

To gain a sense of the quality of our subtractive dataset of conjugates uniquely found in *rpn10Δ* samples, we employed two different assays to evaluate 17 of the 54 candidate Rpn10 substrates. The first and simplest assay was to compare by immunoblotting the level of the candidate protein in wild-type and *rpn10Δ* cells on the assumption that Rpn10 substrates might accumulate to a higher level in *rpn10Δ*. However, we recognized that there may be substrates for which only a small fraction of the total pool is degraded by an Rpn10-dependent pathway, and these substrates might fail this test. Thus, we devised a second assay that measured the level of ubiquitylated candidate protein that was present in wild-type and *rpn10Δ* cells. This second assay allowed us to confirm some candidate proteins (*e.g.* Rpl13) that were not validated by the first assay. Ultimately, we were able to confirm that nearly 60% (10 of 17) of the candidates analyzed are responsive to Rpn10 function. It is important to note that the validation experiments were done with TAP-tagged chromosomal loci (which are in the S288C genetic background), and that the cells were grown in synthetic medium to select for a H$_8$-ubiquitin expression plasmid. By contrast, the affinity purification-mass spec analyses were performed with cells of the W303 strain background grown in rich (YPD) medium. Thus, a failure to confirm a candidate should not be construed as definitive evidence that the candidate is not an Rpn10 ligand. Nevertheless, the apparent high rate of false positives underscores that it is critical to carry out secondary analyses to confirm data acquired in multidimensional MS analyses. Future developments, including the implementation of quantification methods and higher stringency biochemical separations, may reduce the experimental variations and false positive rate.

A previous study (17) from this laboratory revealed that the proteasome substrate receptors Rpn10 and Rad23 can promote degradation of specific subsets of UPS targets and suggested that Rpn10 targets might be restricted to a small class of UPS substrates. However, that study was based on the piecemeal examination of a handful of UPS targets, and it was not designed to reveal the full spectrum of substrates targeted to the proteasome by a given ubiquitin chain receptor. By using the two-step purification multidimensional MS method described here, we have identified several dozen candidate ligands for an Rpn10-dependent targeting pathway that function in a broad range of processes including metabolism, transcription, translation, nuclear transport, and cell cycle. By applying this approach to mutants lacking other receptors (*e.g. rad23Δ*, *dsk2Δ*), it should be feasible to begin the task of constructing a "linkage map" that reveals the spectrum of substrates that are targeted to the proteasome by a specific receptor, which may in turn provide insight into the mechanisms that underlie the allocation of ubiquitylated substrates to different receptor pathways.

---

[3] T. Mayor, J. Graumann, and R. J. Deshaies, unpublished observations.

REFERENCES

1. Weissman, A. M. (2001) Themes and variations on ubiquitylation. *Nat. Rev. Mol. Cell. Biol.* **2,** 169–178

2. Orlicky, S., Tang, X., Willems, A., Tyers, M., and Sicheri, F. (2003) Structural basis for phosphodependent substrate selection and orientation by the SCFCdc4 ubiquitin ligase. *Cell* **112,** 243–256

3. Wu, G., Xu, G., Schulman, B. A., Jeffrey, P. D., Harper, J. W., and Pavletich, N. P. (2003) Structure of a β-TrCP1-Skp1-β-catenin complex: Destruction motif binding and lysine specificity of the SCF(β-TrCP1) ubiquitin ligase. *Mol. Cell* **11,** 1445–1456

4. Semple, C. A. (2003) The comparative proteomics of ubiquitination in mouse. *Genome Res.* **13,** 1389–1394

5. Chau, V., Tobias, J. W., Bachmair, A., Marriott, D., Ecker, D. J., Gonda, D. K., and Varshavsky, A. (1989) A multiubiquitin chain is confined to specific lysine in a targeted short-lived protein. *Science* **243,** 1576–1583

6. Hoege, C., Pfander, B., Moldovan, G. L., Pyrowolakis, G., and Jentsch, S. (2002) RAD6-dependent DNA repair is linked to modification of PCNA by ubiquitin and SUMO. *Nature* **419,** 135–141

7. Hicke, L. (2001) Protein regulation by monoubiquitin. *Nat. Rev. Mol. Cell. Biol.* **2,** 195–201

8. Deveraux, Q., Ustrell, V., Pickart, C., and Rechsteiner, M. (1994) A 26 S protease subunit that binds ubiquitin conjugates. *J. Biol. Chem.* **269,** 7059–7061

9. Hofmann, K., and Falquet, L. (2001) A ubiquitin-interacting motif conserved in components of the proteasomal and lysosomal protein degradation systems. *Trends Biochem. Sci.* **26,** 347–350

10. Fu, H., Sadis, S., Rubin, D. M., Glickman, M., van Nocker, S., Finley, D., and Vierstra, R. D. (1998) Multiubiquitin chain binding and protein degradation are mediated by distinct domains within the 26 S proteasome subunit Mcb1. *J. Biol. Chem.* **273,** 1970–1981

11. Wilkinson, C. R., Seeger, M., Hartmann-Petersen, R., Stone, M., Wallace, M., Semple, C., and Gordon, C. (2001) Proteins containing the UBA domain are able to bind to multi-ubiquitin chains. *Nat. Cell Biol.* **3,** 939–943

12. Rao, H., and Sastry, A. (2002) Recognition of specific ubiquitin conjugates is important for the proteolytic functions of the ubiquitin-associated domain proteins Dsk2 and Rad23. *J. Biol. Chem.* **277,** 11691–11695

13. Kim, I., Mi, K., and Rao, H. (2004) Multiple interactions of rad23 suggest a mechanism for ubiquitylated substrate delivery important in proteolysis. *Mol. Biol. Cell* **15,** 3357–3365

14. Ortolan, T. G., Tongaonkar, P., Lambertson, D., Chen, L., Schauber, C., and Madura, K. (2000) The DNA repair protein rad23 is a negative regulator of multi-ubiquitin chain assembly. *Nat. Cell Biol.* **2,** 601–608

15. Raasi, S., and Pickart, C. M. (2003) Rad23 ubiquitin-associated domains (UBA) inhibit 26 S proteasome-catalyzed proteolysis by sequestering lysine 48-linked polyubiquitin chains. *J. Biol. Chem.* **278,** 8951–8959

16. Hartmann-Petersen, R., Hendil, K. B., and Gordon, C. (2003) Ubiquitin binding proteins protect ubiquitin conjugates from disassembly. *FEBS Lett.* **535,** 77–81

17. Verma, R., Oania, R., Graumann, J., and Deshaies, R. J. (2004) Multiubiquitin chain receptors define a layer of substrate selectivity in the ubiquitin-proteasome system. *Cell* **118,** 99–110

18. Mayor, T., and Deshaies, R. J. (2005) Two-step affinity purification of multiubiquitylated proteins from *Saccharomyces cerevisiae. Methods Enzymol.*, in press

19. Chi, Y., Huddleston, M. J., Zhang, X., Young, R. A., Annan, R. S., Carr, S. A., and Deshaies, R. J. (2001) Negative regulation of Gcn4 and Msn2 transcription factors by Srb10 cyclin-dependent kinase. *Genes Dev.* **15,** 1078–1092

20. Schena, M., Picard, D., and Yamamoto, K. R. (1991) Vectors for constitutive and inducible gene expression in yeast. *Methods Enzymol.* **194,** 389–398

21. Graumann, J., Dunipace, L. A., Seol, J. H., McDonald, W. H., Yates, J. R., 3rd, Wold, B. J., and Deshaies, R. J. (2004) Applicability of tandem affinity purification MudPIT to pathway proteomics in yeast. *Mol. Cell. Proteomics* **3,** 226–237

22. Sadygov, R. G., Eng, J., Durr, E., Saraf, A., McDonald, H., MacCoss, M. J., and Yates, J. R., 3rd. (2002) Code developments to improve the efficiency of automated MS/MS spectra interpretation. *J. Proteome Res.* **1,** 211–215

23. Cherry, J. M., Adler, C., Ball, C., Chervitz, S. A., Dwight, S. S., Hester, E. T., Jia, Y., Juvik, G., Roe, T., Schroeder, M., Weng, S., and Botstein, D. (1998) SGD: *Saccharomyces* Genome Database. *Nucleic Acids Res.* **26,** 73–79

24. Eng, J. K., McCormack, A. L., and Yates, J. R., III (1994) An approach to correlate tandem mass-spectral data of peptides with amino-acid-sequences in a protein database. *J. Am. Soc. Mass Spectrom.* **5,** 976–989

25. McDonald, W. H., Tabb, D. L., Sadygov, R. G., MacCoss, M. J., Venable, J., Graumann, J., Johnson, J. R., Cociorva, D., and Yates, J. R., III (2004) MS1, MS2, and SQT–Three unified, compact, and easily parsed file formats for the storage of shotgun proteomic spectra and identifications. *Rapid Commun. Mass Spectrom.* **18,** 2162–2168

26. Tabb, D. L., McDonald, W. H., and Yates, J. R., 3rd. (2002) DTASelect and Contrast: Tools for assembling and comparing protein identifications from shotgun proteomics. *J. Proteome Res.* **1,** 21–26

27. Piotrowski, J., Beal, R., Hoffman, L., Wilkinson, K. D., Cohen, R. E., and Pickart, C. M. (1997) Inhibition of the 26 S proteasome by polyubiquitin chains synthesized to have defined lengths. *J. Biol. Chem.* **272,** 23712–23721

28. Thrower, J. S., Hoffman, L., Rechsteiner, M., and Pickart, C. M. (2000) Recognition of the polyubiquitin proteolytic signal. *EMBO J.* **19,** 94–102

29. Braun, S., Matuschewski, K., Rape, M., Thoms, S., and Jentsch, S. (2002) Role of the ubiquitin-selective CDC48(UFD1/NPL4)chaperone (segregase) in ERAD of OLE1 and other substrates. *EMBO J.* **21,** 615–621

30. Huibregtse, J. M., Yang, J. C., and Beaudenon, S. L. (1997) The large subunit of RNA polymerase II is a substrate of the Rsp5 ubiquitin-protein ligase. *Proc. Natl. Acad. Sci. U. S. A.* **94,** 3656–3661

31. Minard, K. I., and McAlister-Henn, L. (1994) Glucose-induced phosphorylation of the MDH2 isozyme of malate dehydrogenase in *Saccharomyces cerevisiae. Arch. Biochem. Biophys.* **315,** 302–309

32. Mazon, M. J., and Hemmings, B. A. (1979) Regulation of *Saccharomyces cerevisiae* nicotinamide adenine dinucleotide phosphate-dependent glutamate dehydrogenase by proteolysis during carbon starvation. *J. Bacteriol.* **139,** 686–689

33. Peng, J., Schwartz, D., Elias, J. E., Thoreen, C. C., Cheng, D., Marsischky, G., Roelofs, J., Finley, D., and Gygi, S. P. (2003) A proteomics approach to understanding protein ubiquitination. *Nat. Biotechnol.* **21,** 921–926

34. Hitchcock, A. L., Auld, K., Gygi, S. P., and Silver, P. A. (2003) A subset of membrane-associated proteins is ubiquitinated in response to mutations in the endoplasmic reticulum degradation machinery. *Proc. Natl. Acad. Sci. U. S. A.* **100,** 12735–12740

35. Petroski, M. D., and Deshaies, R. J. (2003) Redundant degrons ensure the rapid destruction of Sic1 at the G1/S transition of the budding yeast cell cycle. *Cell Cycle* **2,** 410–411

36. Meimoun, A., Holtzman, T., Weissman, Z., McBride, H. J., Stillman, D. J., Fink, G. R., and Kornitzer, D. (2000) Degradation of the transcription factor Gcn4 requires the kinase Pho85 and the SCF(CDC4) ubiquitin-ligase complex. *Mol. Biol. Cell* **11,** 915–927

37. Kornitzer, D., Raboy, B., Kulka, R. G., and Fink, G. R. (1994) Regulated degradation of the transcription factor Gcn4. *EMBO J.* **13,** 6021–6030

38. Ghaemmaghami, S., Huh, W. K., Bower, K., Howson, R. W., Belle, A., Dephoure, N., O'Shea, E. K., and Weissman, J. S. (2003) Global analysis of protein expression in yeast. *Nature* **425,** 737–741

39. Wohlschlegel, J. A., Johnson, E. S., Reed, S. I., and Yates, J. R., III (2004) Global analysis of protein sumoylation in *Saccharomyces cerevisiae. J. Biol. Chem.* **279,** 45662–45668

40. Zhou, W., Ryan, J. J., and Zhou, H. (2004) Global analyses of sumoylated proteins in *Saccharomyces cerevisiae.* Induction of protein sumoylation by cellular stresses. *J. Biol. Chem.* **279,** 32262–32268

41. Panse, V. G., Hardeland, U., Werner, T., Kuster, B., and Hurt, E. (2004) A proteome-wide approach identifies sumoylated substrate proteins in yeast. *J. Biol. Chem.* **279,** 41346–41351

42. Rosas-Acosta, G., Russell, W. K., Deyrieux, A., Russell, D. H., and Wilson, V. G. (2005) A universal strategy for proteomic studies of SUMO and

other ubiquitin-like modifiers. *Mol. Cell. Proteomics* **4,** 56–72

43. Zhao, Y., Kwon, S. W., Anselmo, A., Kaur, K., and White, M. A. (2004) Broad spectrum identification of cellular small ubiquitin-related modifier (SUMO) substrate proteins. *J. Biol. Chem.* **279,** 20999–21002

44. Denison, C., Rudner, A. D., Gerber, S. A., Bakalarski, C. E., Moazed, D., and Gygi, S. P. (2005) A proteomic strategy for gaining insights into protein sumoylation in yeast. *Mol. Cell. Proteomics* **4,** 246–254

45. Kanayama, A., Seth, R. B., Sun, L., Ea, C. K., Hong, M., Shaito, A., Chiu, Y. H., Deng, L., and Chen, Z. J. (2004) TAB2 and TAB3 activate the NF-κB pathway through binding to polyubiquitin chains. *Mol. Cell* **15,** 535–548

46. Spence, J., Gali, R. R., Dittmar, G., Sherman, F., Karin, M., and Finley, D. (2000) Cell cycle-regulated modification of the ribosome by a variant multiubiquitin chain. *Cell* **102,** 67–76

47. Schubert, U., Anton, L. C., Gibbs, J., Norbury, C. C., Yewdell, J. W., and Bennink, J. R. (2000) Rapid degradation of a large fraction of newly synthesized proteins by proteasomes. *Nature* **404,** 770–774

48. Turner, G. C., and Varshavsky, A. (2000) Detecting and measuring cotranslational protein degradation *in vivo. Science* **289,** 2117–2120

49. Raasi, S., Orlov, I., Fleming, K. G., and Pickart, C. M. (2004) Binding of polyubiquitin chains to ubiquitin-associated (UBA) domains of HHR23A. *J. Mol. Biol.* **341,** 1367–1379